Pergamon

Tetrahedron, Vol. 53, No. 45, pp. 15495-15513, 1997

0040-4020/97 $17.00 + 0.00

PII: S0040-4020(97)00976-9

A Contemporary Survey of Covalent Connectivity and Complexity. The Divergent Synthesis of Poly(thioether) Dendrimers. Amplified, Genealogically Directed Synthesis Leading to the de Gennes Dense Packed State

Mary K. Lothian-Tomalia, David M. Hedstrand and Donald A. Tomalia*

Michigan Molecular Institute, 1910 W. St. Andrews Road, Midland, MI 48640

Anne Buyle Padias* and H.K. Hall, Jr.

C.S. Marvel Laboratories, Chemistry Department, The University of Arizona, Tucson, AZ 85721

Abstract: A new poly(thioether) dendrimer (d-PTE) family is synthesized using preformed branch cell reagents (BCR) in a "genealogically directed syntheses" (GDS) strategy. Bicyclic orthoester functionality is introduced into a branch cell reagent (BCR) to temporarily mask pentaerythritol derived branch cells which are used to construct the interior of this new dendrimer family. These BCRs with multiplicities =3 (N_b=3), are organized and amplified around an initiator core with multiplicity = 4 (N_c=4). The initiator core, pentaerythritol tetrabromide (N_c= 4), is allowed to react with four equivalents of 4-acetothiomethyl-2,6,7-trioxabicyclo[2.2.2]octane (N_b= 3) in the presence of base, to form the first generation possessing four bicyclic orthoester groups. After deprotection and transformation to bromide surface groups *via* tosylate intermediates, the second generation possessing twelve bicyclic orthoester groups is formed. Surprisingly, attempted displacement of all 36 surface groups at the third generation level showed that only one third of the end groups could be substituted. These experimental data suggest that this (N_c=4, N_b=3) type dendrimer family exhibits de Gennes dense packing properties at the third generation level. Elemental analysis, FTIR, H/C ^{13} nmr spectroscopy and mass spectroscopy were used to confirm the structures. Molecular simulation data suggest that this dendrimer family should not undergo de Gennes dense-packing until the fourth generation. Steric requirements of the bulky mercaptomethyl anion used in the S_N2 displacement of terminal bromides on this congested surface are proposed as the reason for incomplete formation of the third generation. This observation illustrates another example of "sterically induced stoichiometry" (SIS).

INTRODUCTION

From a mathematical/phenomenological perspective, examination of the total number of covalent bonds formed and the mode of bond formation in a reaction sequence provides an interesting criterion by which to define broad classes of molecular structure and complexity. This has important implications as one ponders the natural origin of buckministerfullerene (C_{60}), the primordial protein/nucleic acid structures or the complex hydrocarbons found in coal/oil reserves. What is the chemical genealogy of these materials? Are these structures assembled from larger preformed modules in relatively few bond formation steps or are small modules implemented in many bond formation steps? Are there new synthetic strategies yet to be defined? Using this simple perspective, synthetic covalent chemistry can be generally classified into the following three recognizable areas:[1]

Covalent Synthesis

I.	II.	III.
(1828 - Present)	(1930's - Present)	(1979 - Present)
Traditional Organic Chemistry[2]	Traditional Polymer Chemistry[3-4]	Dendritic Macromolecular Chemistry[5-6a,b]
(a) *Incremental* number of covalent bonds formed using classical reagents. (b) Relatively small (i.e., < 1nm) molecules formed. Precise control of size, shape, mass, functional groups, topology and flexibility.	(a) *Large (multiple)* numbers of bonds formed using reactive monomers. (b) Large molecules (i.e., > 1nm) formed. Statistical distribution of products as a function of size and mass. Some control of topology and flexibility. Virtually no control of shape.	(a) *Exponential* numbers of covalent bonds formed using branch cell reagents. (b) Large molecules (i.e., >1nm) formed. Precise control of size, shape, mass, functional groups, topology and flexibility.

Figure 1

This paper describes an example of the third class of covalent synthesis; *dendritic macromolecular chemistry*.[7a-d] A new poly(thioether) dendrimer family is synthesized using preformed branch cells in a "genealogically directed synthesis" (GDS) strategy[7b] with covalent bond amplification. Before discussing these details, it is appropriate to compare and contrast these three types of covalent syntheses.

I. Traditional Organic Chemistry

Historically, synthetic bond formation leading to covalent molecular structures has progressed through the above three well defined stages. The first phase involved incremental combinations of carbon and specific heteroatoms to produce key hydrocarbon building blocks (modules) and functional groups (connectors), respectively. Atomic level building components required for the construction of these modules involved all three hybridization states of carbon. In retrospect, the resulting modules appear to fall into at least five distinct architectural categories (topologies), based on covalent connectivity[2,8] (see Figure 2).

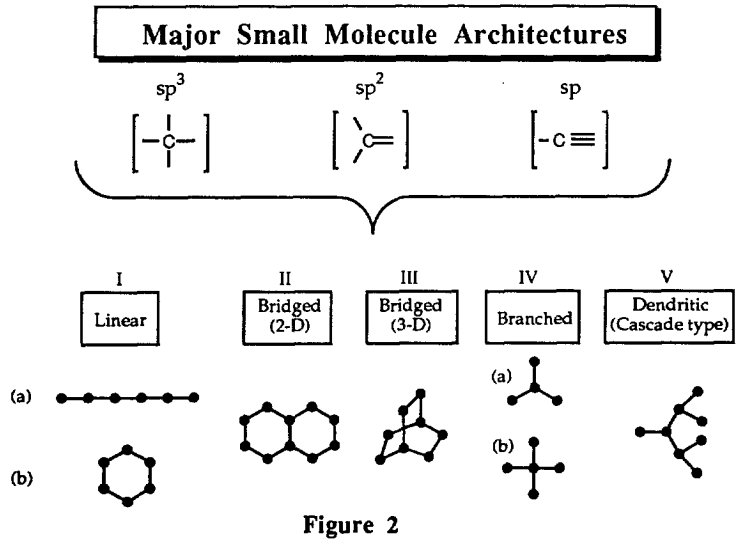

Figure 2

Combinations of various heteroatoms with and without carbon, provided an enormous variety of functional groups. These substitutions, of course, influence and define the reactivity, polarity, solubility, and many other physical properties of these modules; however, their most important role has been as reactive connectors for covalent bond formation. This function has allowed the assembly of literally millions of more complex structures by either; (a) divergent or (b) convergent strategies involving multiple, step-wise, bond formation steps followed by product isolation at each stage. These strategies are recognized as the essence of traditional organic synthesis.

(a) Divergent Multistep Synthesis

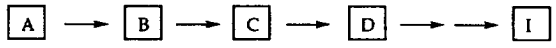

(b) Convergent Multistep Synthesis

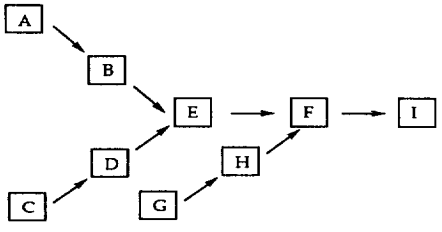

The general field of Merrifield synthesis[9a-d] is an example of the divergent strategy which involves chronological introduction of precise amino acid sequences to produce a linear architecture. It may be thought of as a "linear, genealogically directed synthesis" (L-GDS), since the molecular ancestry leading to product ∎ may be chronologically determined by " linear retrosynthetic analysis."[2]

Many examples of the convergent strategy can be found in contemporary approaches to natural product synthesis. Most of these routes to target molecules are devised by retrosynthesis from the final product.[2] This involves the transform of the target molecule to simpler building blocks as one reduces the intermediates leading to product in both molecular size and complexity. Since many possible approaches may be conceived, these strategies do not have well defined molecular genealogy. Mathematically, at least one covalent bond or in some cases several bonds may be formed per reaction step (N_i). Assuming high yield reaction steps and appropriate isolation stages, one can expect to obtain precise monodisperse products. In either case, the total number of covalent bonds formed can be expressed as follows:

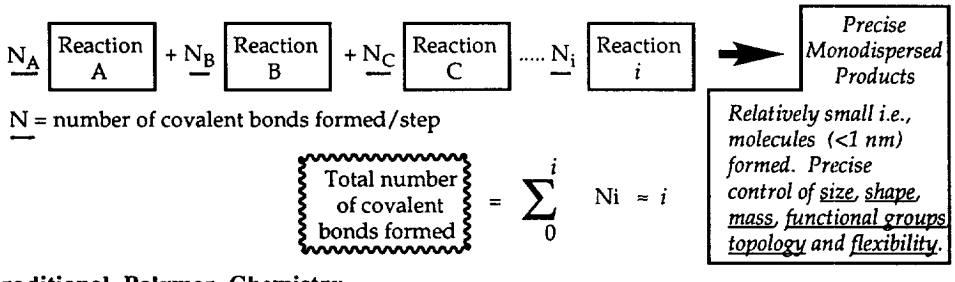

II. Traditional Polymer Chemistry

A second type of covalent synthesis has evolved around the use of reactive modules (AB-type monomers) that can be engaged in multiple covalent bond formation to produce single molecules. Such multiple bond formation is driven either by chain reaction or poly(condensation) schemes. Staudinger first introduced this paradigm in the 1930's[3] by demonstrating that reactive monomers could be used to produce a statistical distribution of one dimensional molecules with very high molecular weights (i.e., > 10^6 daltons). These covalent synthesis protocols underpin the science of traditional polymerizations. As many as 10,000 or more covalent bonds can be formed in a single chain reaction of monomers. Although megamolecules with nanoscopic dimensions may be attained, relatively little opportunity is offered with these methods to precisely control critical molecular design parameters such as sizes, atom positions, covalent connectivity (i.e., other than linear topologies) or molecular shapes.

These polymerizations usually involve AB-type monomers based on substituted ethylenes, strained small ring compounds or AB-type monomers which may undergo polycondensation reactions. The chain reactions may be initiated by free radical, anionic or cationic initiators.

$$n\,[AB]\ (monomers) \longrightarrow \sim\{AB\}_n$$

Multiple covalent bonds are formed per chain sequence; wherein, the average lengths are determined by monomer to initiator ratios. Generally, polydispersed structures are obtained which are statistically controlled. If one views these polymerizations as extraordinarily long sequences of individual reaction steps, the average number of covalent bonds formed/chain can be visualized as follows:

$$\underline{N}_A\left(\frac{M}{I}\right)\boxed{\text{Reaction A}} + \underline{N}_B\left(\frac{M}{I}\right)\boxed{\text{Reaction B}} \ldots\ldots \underline{N}_i\left(\frac{M}{I}\right)\boxed{\text{Reaction } i} \longrightarrow \boxed{\textit{Polydispersed Products}}$$

Where: $\frac{M}{I}$ = monomer: initiator ratio; $\underline{N}$ = number of covalent bonds formed/step

$$\boxed{\text{Average number of covalent bonds formed}} = \sum_0^i Mi/I \approx \frac{\Sigma Mi}{I}$$

Large molecules, (i.e., >1nm) formed. Statistical distribution of products as a function of size and mass. Some control of topology and flexibility. Virtually no control of shape.

All three classical polymer architectures; namely, Class I *Linear*, Class II *Cross-linked (bridged)* and Class III *Branched* topologies can be prepared by these methods (see Figure 3), keeping in mind that simple introduction of covalent bridging bonds between polymer chains (Class I type) is required to produce Class II cross-linked (thermoset) type systems.[10, 16]

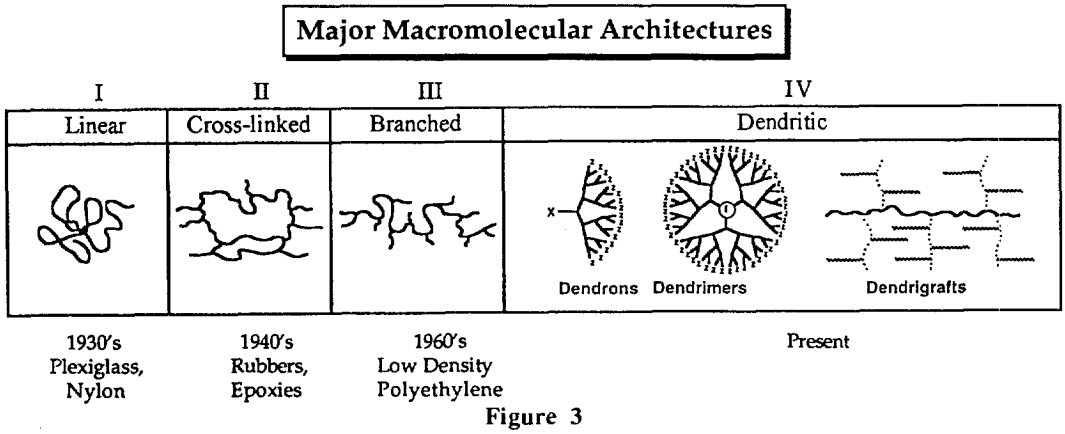

Figure 3

It should be noted that these major macromolecular topologies completely parallel those noted for small molecule architectures (see Figure 2).

III. Dendritic Macromolecular Chemistry

More recently, new strategies have been developed which now allow amplified covalent bond formation as a power function of reaction steps. By using these methods, a fourth new class of polymers has been synthesized which are referred to as "dendritic macromolecules." Just as we have noted earlier for simple organic structures, dendritic molecules can be synthesized by either (a) divergent[5] or (b) convergent strategies[11-12] as described below:

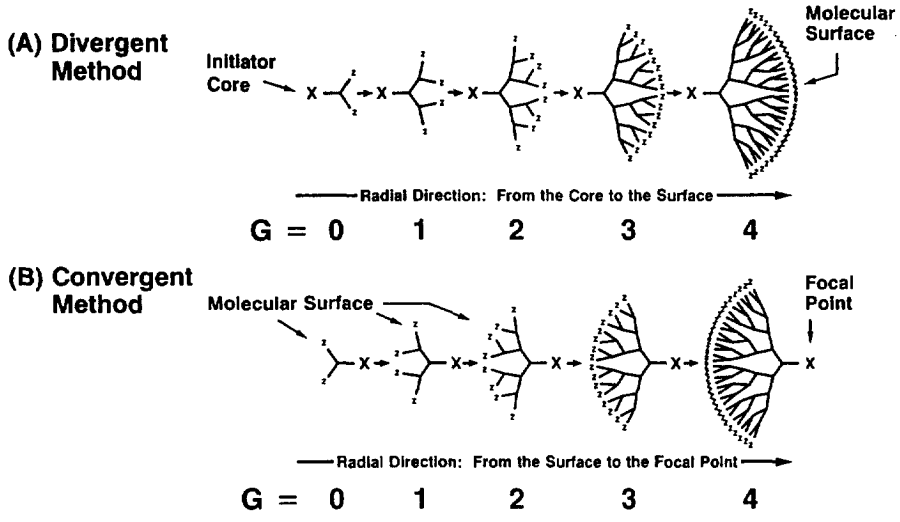

Figure 4

This work will focus solely on the divergent approach which involves either (a) the *in situ* construction of branch cells around an initiator core or (b) the covalent coupling of preformed branch cells (BC) (derived from branch cell reagents, BCR's) around such an attractor. A monovalent core produces tree-like assemblies (*dendrons*); whereas, polyvalent cores yield multiples of these assemblies (*dendrimers*). Depending on the multiplicity of the core (N_c) and the branch cells (N_b), one can produce a wide variety of precise macromolecular architectures with exponential numbers of reactive surface groups. Two dimensional projections illustrate a tetra-dendron dendrimer series, with $N_c = 4$ and $N_b = 3$. Each reaction step is referred to as a *generation* (Figure 5).

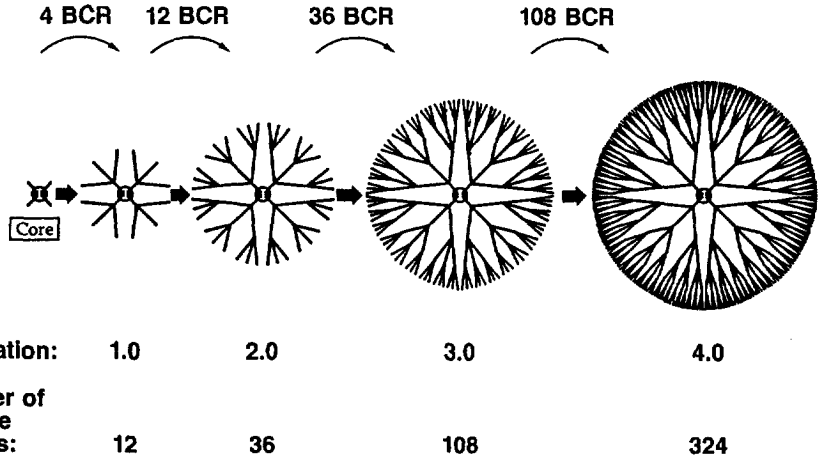

Figure 5

These dendrimer constructions follow precise mathematical rules and principles.[5] As such, one can predict certain parameters and then experimentally test them by a variety of analytical methods including: titration, mass spectroscopy, infrared and NMR spectroscopy. Mathematically, the number of surface groups, number of covalent bonds formed and precise molecular weights as a function of reaction steps (generations) can be calculated according to the following expressions:

$$\text{Number of Surface Groups} \quad : \quad Z = N_c N_b^{G}$$

$$\text{Number of Branch Cells} \quad : \quad BC = N_c\left[\frac{N_b^{G}-1}{N_b-1}\right] = \text{Number of Covalent Bonds Formed/Generation}$$

$$\text{Molecular Weights} \quad : \quad MW = M_c + N_c\left[M_{RU}\left(\frac{N_b^{G}-1}{N_b-1}\right) + M_t N_b^{G}\right]$$

Dendrons and dendrimers possess three distinct architectural components, namely a *core*, *interior* and *surface groups*. As such, the structural notations for the present poly(thioether) dendrimer family may be expressed as follows:

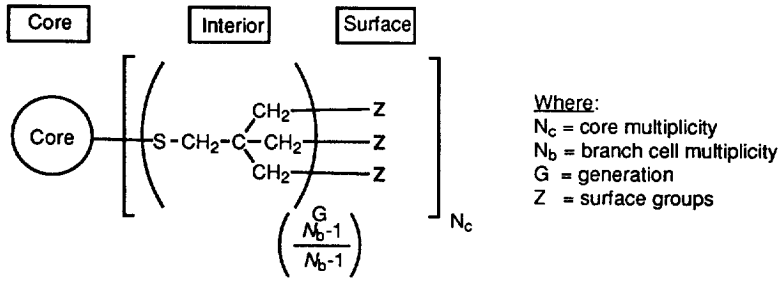

Figure 6

As opposed to the *linear, genealogically directed synthesis* (L-GDS) exemplified by Merrifield poly(peptide) or poly(nucleic acid) synthesis, one may think of divergent dendron and dendrimer approaches as examples of *amplified, genealogically directed synthesis*, (A-GDS). Amplification occurs according to the dendritic math rules described above. The genealogy of the dendritic construct is determined by the *core*, *generational sequence of the interior* and the *terminus* (surface) of the completed structures. The genealogical components are illustrated in Figure 7 and their significance is described in greater detail elsewhere.[7b]

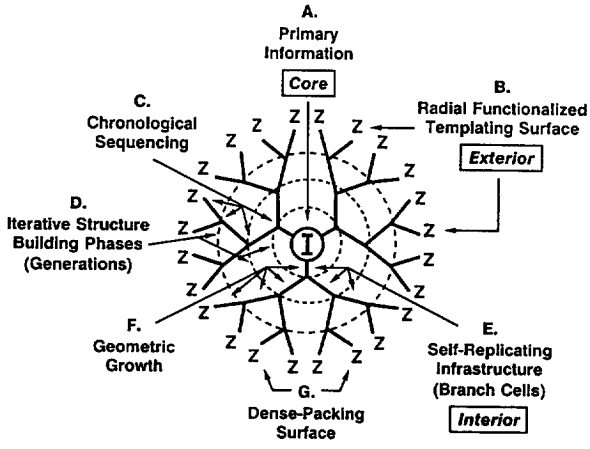

Figure 7

It is readily apparent that these abiotic molecular level (A-GDS) strategies have many things in common with biological systems. Certain biological processes, such as polymerase chain reactions (PCR)[13] or cell mitosis[14] may be thought of as analogous examples of amplification, but at much larger dimensional scales than are found in dendrimers (see Figure 8).[15]

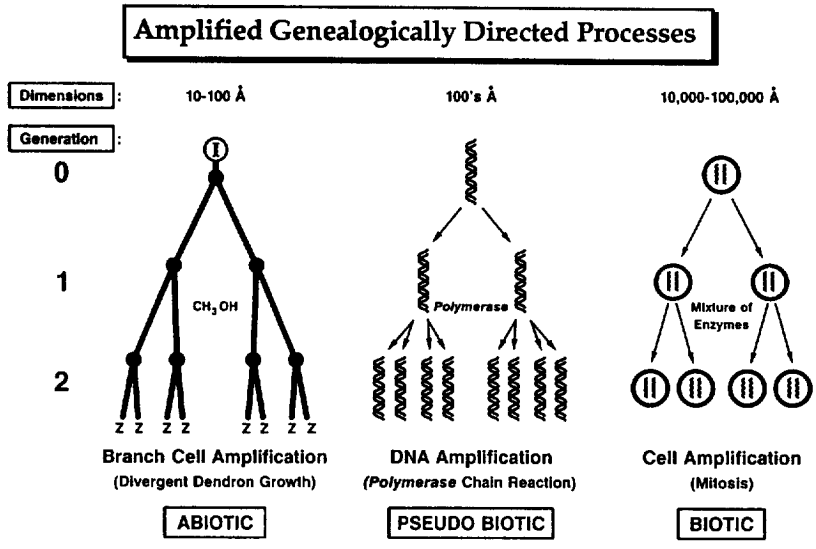

Figure 8

Mathematically, the number of covalent bonds formed per generation (reaction step) in a dendron/dendrimer synthesis varies as a power function of the reaction steps, as illustrated below. This analysis shows that covalent bond amplification occurs in all dendritic synthesis strategies. This feature clearly differentiates dendritic processes from covalent bond synthesis found in traditional organic chemistry or polymer chemistry.

$$\underline{N_c}\boxed{\text{Reaction A}} + \underline{N_cN_b}\boxed{\text{Reaction B}} + \underline{N_cN_b^2}\boxed{\text{Reaction C}} \;\ldots\; \underline{N_cN_b^{i-1}}\boxed{\text{Reaction } i} \Rightarrow \textit{Precise Monodispersed Products}$$

Large molecules (i.e., >1 nm) formed. Precise control of size, shape, mass, functional groups, topology and flexibility.

Where: $\underline{N_c}$ = initiator core multiplicity; $\underline{N_b}$ = branch cell multiplicity;

$\underline{N_cN_b^{i-1}}$ = number of covalent bonds formed/step

$$\text{Total number of covalent bonds formed} = \sum_{x=0}^{i-1} N_cN_b^x = N_c\left[\frac{N_b^{i}-1}{N_b-1}\right]$$

It is interesting to note, that this same mathematical analysis may be used to predict the amplification of DNA by PCR methods or the proliferation of biological cells by mitosis as a function of generation. The biotic examples, of course, multiply according to the familiar geometric progression; 2^G, where: G = generation or number of reaction reiteration (synthetic proliferation). It shall be noted that each of the three amplified, genealogical directed processes are initiated by a primary information source or template. In the case of the dendron, it is the *initiator core* and for PCR amplification it is the *primary DNA sequence*; whereas, for cell mitosis, it is the *stem* or *germ cell* that are required to begin the process. In all three cases, these processes involve the transformation and amplification of important information from the source to the termini of these respective geometric progressions, but at different size scales. Several important features that differentiate

dendron amplification from the two biological processes is that this information is transferred to the termini (surface groups) *via* covalent connectivity between the branch cells. These covalently derived, information conduits are further modulated by the size, composition and bond angles of the constituent branch cells. They literally determine the final covalent infrastructure of the resulting dendron/dendrimer molecule. The two related biological processes, on the other hand, transfer their primary information by templating events to produce decoupled, but yet amplified products that continue the progression by carrying this information to the next generational level.

IV. *Linear* and *Amplified* - Genealogically Directed Synthesis

Genealogically directed synthesis (GDS) was first proposed and broadly defined earlier by one of us (DAT) to describe unusual sequencing and information storage patterns observed in dendritic macromolecular constructs.[7b,15] *It was defined as those synthetic strategies that involve an ordered sequence of chronological reaction steps (generations); wherein, critical intermediates involved in the sequence (molecular ancestry), function as templates upon which subsequent structural components are introduced, usually in some chronological order. Actually the critical sequencing order is determined by the molecular positions of the sequenced units relative to the genesis (initiator point), the terminus, as well as relative interior positions defined by the completed covalent structure. Deviations (errors) from a desired order or ideality in the sequence are referred to as structural mutations. Experimental documentation of such structural mutants has been reported.*[19]

Prime examples of linear, genealogically directed synthesis (L-GDS) may be observed in both synthetic and biologically derived poly(peptide) (protein)[9a-d] and poly (nucleic acid) synthesis.[16] Using these strategies, important molecular information can be chronologically sequenced and stored within the resulting covalent constructs. As a consequence, structural errors and/or ideality are recorded by virtue of their covalent connectivity. The importance of (L-GDS) can be recognized by reviewing the well known biotic strategy for controlling natural macromolecule structures such as DNA → *m*-RNA leading to precise protein constructs.[16]

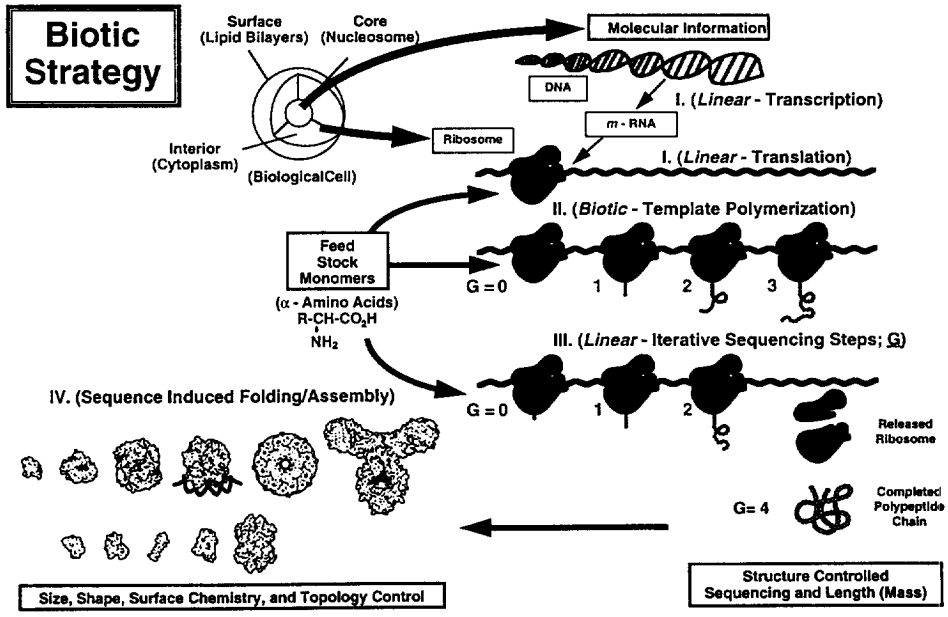

Figure 9

Linear transcription of molecular information from DNA to m-RNA involves a (L-GDS) process; wherein, a template strand of DNA transfers complementary sequence information to allow the linear synthesis of a *m*-RNA copy. It should be noted that the (L-GDS) starts at the free 5'-end of the chain and proceeds toward the free 3'-end or terminus. Figures 10a-b show the linear nucleic acid sequences and codon triplets, respectively, that are required for linear transcription and translation from DNA → *m*-RNA → linear protein structures. As shown in

Figure 9, the transcribed m-RNA codon sequences are translated by means of codon directed template polymerizations in the ribosomes of biological cells. This translation is a linear, iterative sequencing process that occurs in discrete steps (generations). Translations of m-RNA codon sequences to protein sequences is also a (L-GDS) process involving first a promoter (initiator) sequence. This sequence usually requires a group of six base pairs preceding the bases that specify α-amino acid sequences in the primary protein structure followed by three codons that specify termination of the peptide synthesis. Several of these termination codons are illustrated in Figure 10.

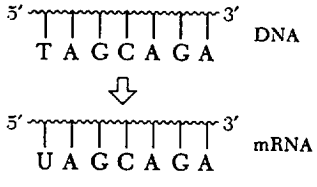

TTA	Leu	TCT	Ser	CGT	Arg						
TTG		TCC		CGC							
CTT		TCA		CGA							
CTC		TCG		CGG							
CTA		AGT		AGA							
CTG		AGC		AGG							
GTT	Val	CCT	Pro	ACT	Thr	GCT	Ala	GGT	Gly		
GTC		CCC		ACC		GCC		GGC			
GTA		CCA		ACA		GCA		GGA			
GTG		CCG		ACG		GCG		GGG			
ATT	Ile	TAA	signal for termination of the peptide chain								
ATC		TAG									
ATA		TGA									

(a) A section of template DNA coding strand required to synthesize a *m*-RNA copy in a DNA → *m*-RNA transcription.

(b) Various nucleic acid codons (triplets) required for encoding α-amino acid sequences in the translation of *m*-RNA → poly(peptides)

Figure 10

In summary, critical architectural and functional molecular information originates from the nucleosome (core) of biological cells. It is stored as a linear molecular document (DNA) in the cell core, then transferred to the cytoplasm (interior) where it is converted within the ribosome into architectural and functional proteins. Many of these proteins migrate from or modulate the lipid bilayer (surface) encasement of the biotic cells. These proteins are 3-D molecular messages or information that precisely define the *size*, *shape* and *general properties* of the cells (i.e., a liver versus pancreas cell and how cells communicate with each other). This articulate information flow involves precise covalent synthesis and information storage based on at least three well recognized *linear*-GDS types. These three GDS reaction types are: (I) *replication*-L-GDS; (II) *transcription*-L-GDS and (III) *translation*-L-GDS as described in Figure 11a. It should be noted that the transfer of information between these L-GDS processes and storage sites, usually occurs by non-bonding, complementary, recognition events.

Amplified-GDS processes associated with divergent dendrimer synthesis involves a similar flow of molecular level information, however, it occurs completely within the dendrimer structure. This information flows from the core, through the interior branch cell domain to the surface (terminal) functionality by means of the dendritic covalent connectivity. This information path architecturally parallels that observed in biotic cells (i.e., core → interior → surface). It should be noted that the chronological ordering of this information within a dendrimer (i.e., generation to generation) is similar to the linear chronological ordering of nucleic acids or ∝–amino acids in each of the biotic I - III-L-GDS processes. A major difference associated with A-GDS is the ability to amplify covalent bonds formed, the molecular mass of the structure as well as the number of surface groups with this process. This of course, is directed according to mathematically driven dendritic power functions dependent on N_c and N_b. This amplified information defines important dendrimer parameters; such as, *size, shape, surface groups density*, etc. all of which are contained within each dendrimer structure as described in Figures 11b and 13 (see Discussion Section). It should be noted that although the two molecular information flow patterns found in cells and dendrimers have many features in common, their respective communication paths are orders of magnitude different in size scale (i.e., <10nm in dendrimers and >1000nm in biotic cells (see Figure 11 a & b).

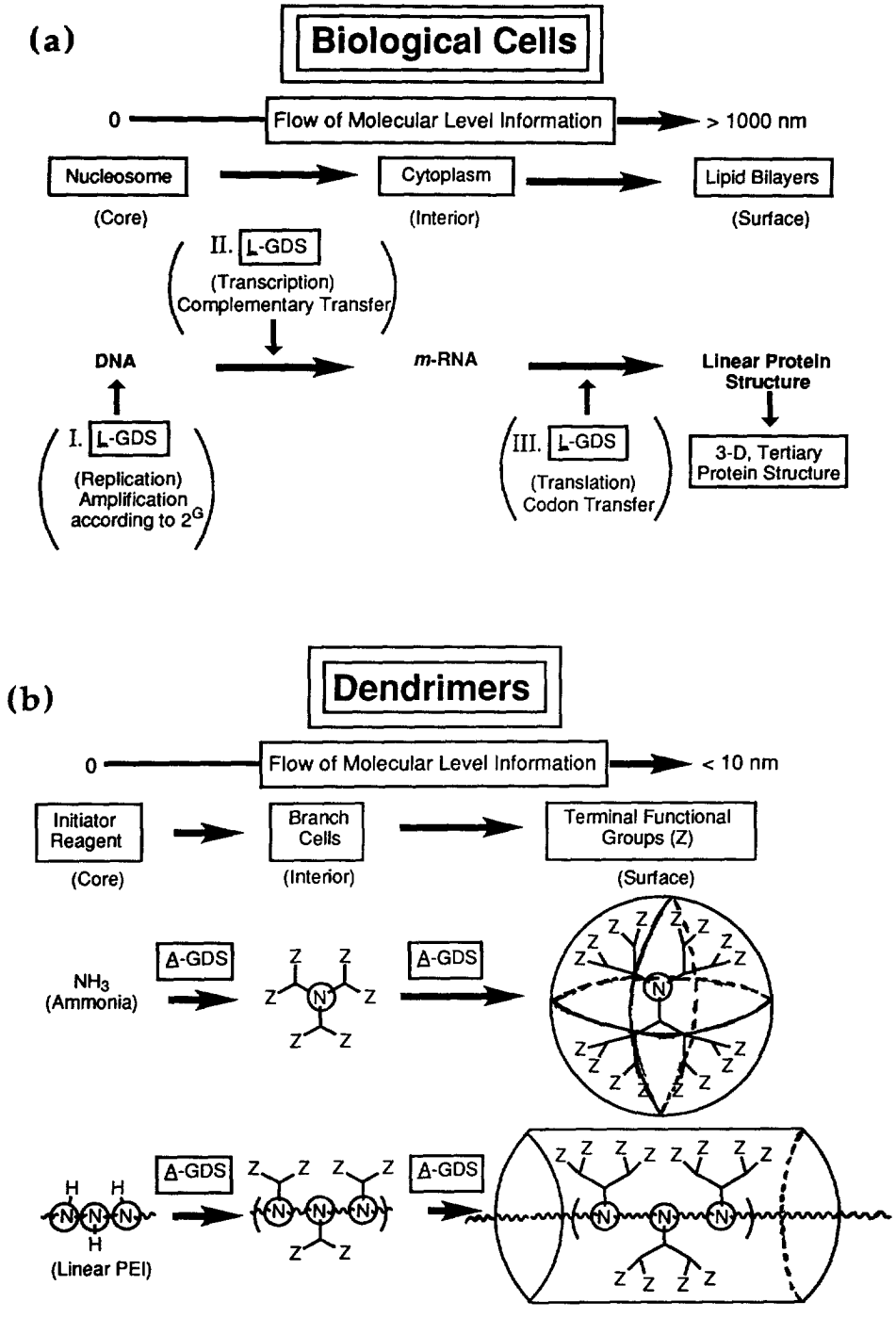
(a)
Biological Cells
0
Flow of Molecular Level Information
> 1000 nm
Nucleosome
(Core)
Cytoplasm
(Interior)
Lipid Bilayers
(Surface)
II. L-GDS
(Transcription)
Complementary Transfer
DNA
m-RNA
Linear Protein Structure
I. L-GDS
(Replication)
Amplification
according to 2^G
III. L-GDS
(Translation)
Codon Transfer
3-D, Tertiary Protein Structure
(b)
Dendrimers
0
Flow of Molecular Level Information
< 10 nm
Initiator Reagent
(Core)
Branch Cells
(Interior)
Terminal Functional Groups (Z)
(Surface)
NH3
(Ammonia)
A-GDS
A-GDS
A-GDS
A-GDS
(Linear PEI)

Figure 11

RESULTS

I. Branch Cell Reagent Synthesis

A synthetic strategy similar to that reported earlier by us for poly(ether) dendrimers[17] was used successfully for this dendrimer family. The bicyclic orthoester functionality was utilized to mask triads of hydroxyl groups on neopentyl moieties, thus generating pivotal branch cell reagent, 4-acetothiomethyl-2,6,7-trioxabicyclo [2.2.2.]octane (ATBO). Initially, we attempted to hydrolyze ATBO and isolate the reactive branch

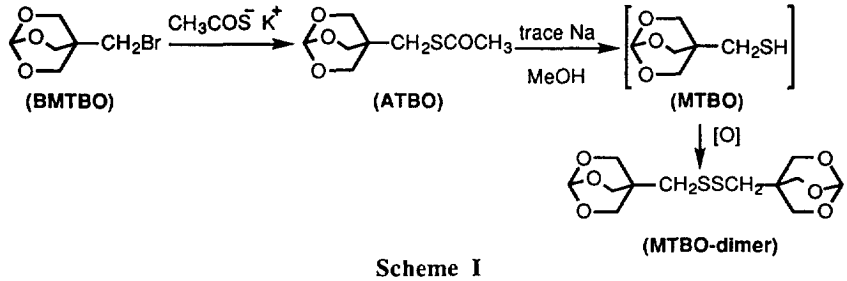

Scheme I

cell reagent; 4-mercaptomethyl-2,6,7-trioxabicyclic [2.2.2] octane (MTBO) by use of trace sodium metal in methanol. This intermediate, however, was found to be too susceptible to oxidation and was best utilized by generating it *in situ*. Simply combining ATBO with potassium *t*-butoxide in glyme, provided a suitable protocol for generating MTBO anion in the presence of dendritic bromide intermediates without competitive side reactions from the base reagent. The MTBO disulfide was deliberately synthesized with ease, by bubbling oxygen through a reaction mixture containing MTBO. All spectral data for the mercaptan and disulfide were essentially identical. A single property that distinguished the two materials from each other was the melting point (i.e., 180°C for the disulfide compared to 78°C for MTBO).

II. Branch Cell Reiteration/Amplification Strategy

Mathematically defined stoichiometries of branch cell reagent (BCR) as illustrated in Figure 5, were used to synthesize dendritic poly(thioethers) (d-PTE); generations 1 -3. The synthetic amplification was initiated from a pentaerythritol tetrabromide core, ($N_c = 4$), using protected MTBO, ($N_b = 3$) as the reactive BCR. Branch cell reiteration was a four step process involving (a) nucleophilic displacement of bromide ion by mercaptide functionality, (b) mild acid hydrolysis of the bicyclic orthoester group to deprotect three hydroxyl groups/orthoester moiety, (c) tosylation of the hydroxyl groups and finally (d) bromide ion displacement of the tosylate groups to return the (A-GDS) sequence to the next generational level. This reaction sequence is as illustrated in Scheme II.

First Generation (Scheme II) - Oxidation problems were avoided with the mercaptan derivative or the (MTBO) sulfide anion, by generating the (MTBO) sulfide anion *in situ*. Potassium t-butoxide in glyme provided an alkaline reaction mixture for liberation of the MTBO sulfide anion without side reaction of the bromide function in the neopentyl positions. This reaction is heterogeneous, however, no massive amounts of salt precipitated. Once t-butoxide is mixed with glyme, both the thioacetate ATBO and pentaerythritol tetrabromide can be added as solids concurrently. A slight excess of the thioacetate was used to ensure complete reaction. *The reaction has to be run with strict exclusion of oxygen*. Any sulfide anion that is formed in the presence of base is very reactive and will easily dimerize to the disulfide. Furthermore, it is also very difficult to separate disulfide byproducts from the dendrimers by recrystallization. After four hours of refluxing in glyme (80°C), complete reaction is obtained. Methyl iodide is added to the reaction mixture before work-up to remove excess MTBO reagent which is much more soluble. All spectral and analytical data indicate that the product obtained; (d-PTE-$(BO)_4$) is pure.

Hydrolysis of the tetra-bicyclic orthoester d-PTE-$(BO)_4$ is performed exactly as described earlier for the poly(ether) dendrimers.[17] The product is mixed with acidic methanol, and a mixture of methanol and methyl acetate is slowly distilled off. A white solid is obtained, whose spectral data correspond to the proposed structure. The transformation of dodeca-alcohol d-PTE-OH_{12} to the dodeca-tosylate (d-PTE-$(Tos)_{12}$) was performed using tosyl chloride in pyridine for 5 days at room temperature. After recrystallization, all spectral and analytical data are in agreement with the proposed structure.

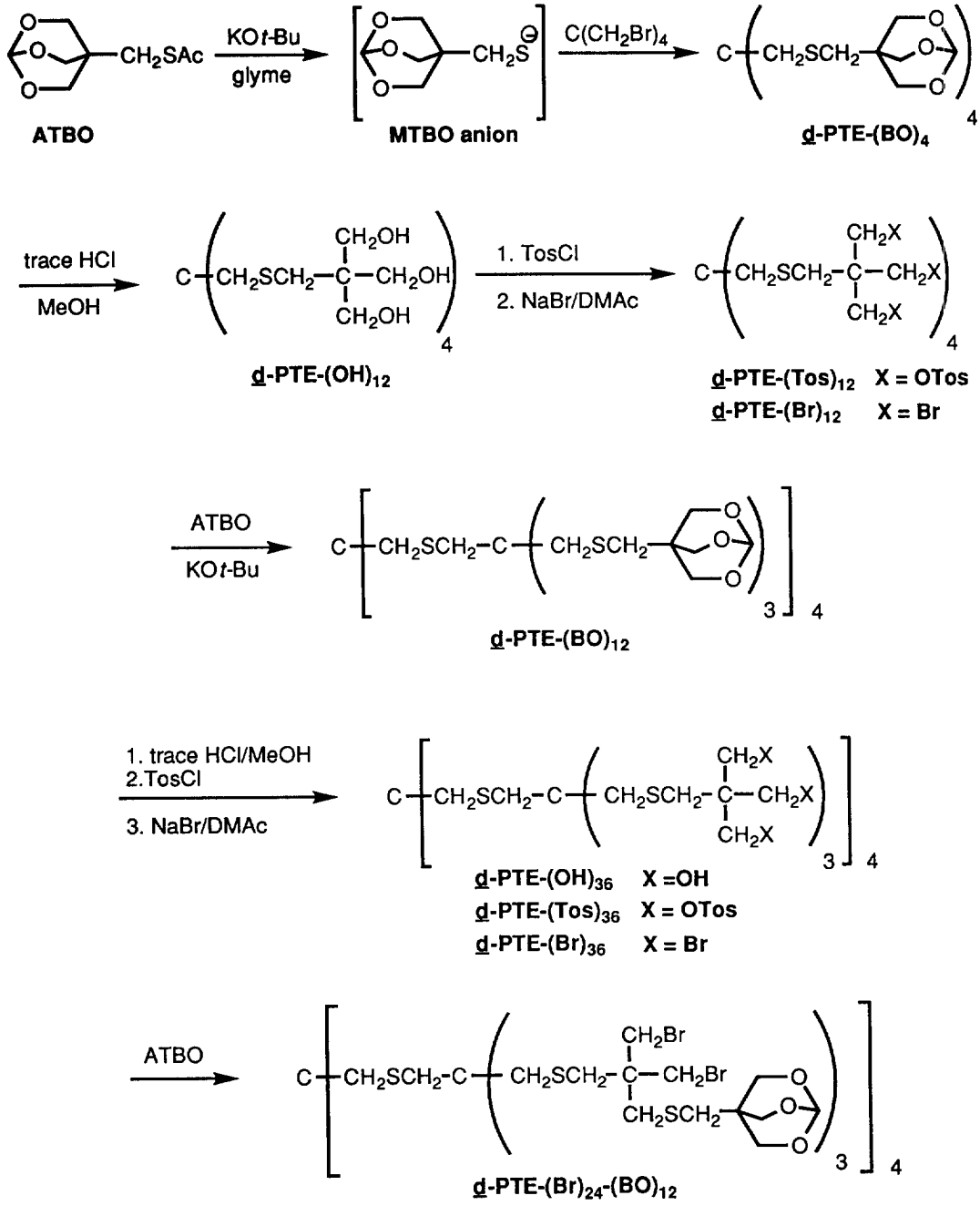
KO*t*-Bu
glyme
C(CH2Br)4
ATBO
MTBO anion
d-PTE-(BO)4
trace HCl
MeOH
1. TosCl
2. NaBr/DMAc
d-PTE-(OH)12
d-PTE-(Tos)12 X = OTos
d-PTE-(Br)12 X = Br
ATBO
KO*t*-Bu
d-PTE-(BO)12
1. trace HCl/MeOH
2.TosCl
3. NaBr/DMAc
d-PTE-(OH)36 X =OH
d-PTE-(Tos)36 X = OTos
d-PTE-(Br)36 X = Br
ATBO
d-PTE-(Br)24-(BO)12

Scheme II

Conversion of the tosylates to the dodeca-bromide d-PTE-$(Br)_{12}$, involved an identical procedure to that used for the poly(ether) dendrimer synthesis.[17] d-PTE-$(Tos)_{12}$ is mixed with excess sodium bromide in dimethyl acetamide and heated at 150°. The mixture is kept at this temperature for only 1 hour, and then poured into ice water. The dodecabromide precipitates in high yield (85-90%). These multibromides are very insoluble and could not be purified successfully by recrystallization. They were used without further purification.

The purity of the intermediates and the extent of reaction could be easily determined by integration of the ^{1}H-NMR spectra. The purity of these compounds was then confirmed by ^{13}C-NMR, elemental analysis and FAB-mass spectrometry.

Second generation (Scheme II) - Reaction of the dodecabromide, d-PTE-$(Br)_{12}$ with twelve equivalents of ATBO in the presence of base did not proceed in a satisfactory manner. Incomplete reactions were usually obtained, even if excess thioacetate derivative was used. Higher temperatures could not be used since an experiment run in diglyme at 160° under identical conditions used for the d-poly(ethers) caused product decomposition.

More complete reactions were obtained by adding two consecutive batches of ATBO and potassium t-butoxide. The first batch consisted of 14 equivalents of the two components which was then refluxed for four hours, after which another 7 equivalents were added, and the reflux was continued overnight. After quenching with methyl iodide, d-PTE-$(BO)_{12}$ was obtained in rather low yield (~ 40%), but this product was pure after precipitation and all spectral data indicated complete reaction.

Subsequent reaction steps to produce subshells within the generation = 2 shell did not pose any special problems. The bicyclic orthoester functions d-PTE-$(BO)_{12}$ hydrolyzed smoothly to form 36-dendri: methane[4]: d-PTE-$(OH)_{36}$, which was then transformed to the dendrimer possessing 36 tosylate groups, d-PTE-$(Tos)_{36}$. Major resonance bonds in the ^{1}H-NMR spectrum of d-PTE-$(Tos)_{36}$ show substantial broadening compared to the spectrum of the dodeca-tosylated: PTE-$(Tos)_{12}$. This is rather surprising, since computer assisted molecular simulations did not predict extraordinary crowding at this point.

Conversion of d-PTE-$(Tos)_{36}$ to (d-PTE-$(Br)_{36}$) also proceeded smoothly in high yield. No residual tosylate groups could be detected by NMR spectroscopy. Chemical bromine analysis indicates that the substitution occurs to give d-PTE-$(Br)_{34}$.

Third generation (Scheme II) - In our hands it was not possible to form ideally amplified third generation d-PTE-$(BO)_{36}$. Using the two-step sequential addition of base and thioacetate derivative, did not produce any ideally amplified products. At first, a batch of KOtBu and ATBO (40 equivalents) was mixed with PES-$(Br)_{36}$ in glyme and refluxed for four hours; then another batch of KOtBu and ATBO was added (20 equivalents), and the mixture was refluxed overnight under argon atmosphere. The excess sulfide anion was quenched with methyl iodide. NMR of the product indicates that only 12 bicyclic orthoester functionalities were introduced in the dendrimer, *even after using 60 equivalents of reagent*!

III. Mass Spectral Analysis of the Dendrimers

Due to the symmetry of these dendrimers, NMR and IR spectral analyses look essentially equivalent for the various generational levels. Mass spectra on the other hand, give precise molecular weight information to compare with mathematically predicted molecular masses. All reaction intermediates were analyzed by Fast Atom Bombardment Mass Spectrometry (FAB/MS). The bicyclic orthoester terminated dendrimers, d-PTE-$(BO)_4$ and d-PTE-$(BO)_{12}$ caused some complication due to the insolubility in the polar FAB matrix.

On the other hand, d-PTE-$(OH)_{12}$ exhibited a positive and negative ion FAB mass spectrum in the predicted molecular ion region, thus demonstrating that the desired compound was indeed obtained. A protonated molecular ion $(M+H)^+$ was observed at m/z 673 in the positive spectrum, while a complementary deprotonated molecular ion is observed at m/z 671 in the negative ion spectrum. Typical water loss fragments associated with alcohols were observed.

Dendri-PTE-$(Tos)_{12}$ (MW 2519) was analyzed by field desorption, however, the signal was not very intense. The predicted molecular species were observed and displayed the expected isotope cluster. No serious byproducts were noted. The M-169 fragment observed, indicates the loss of a tosyl group reverting back to a stable tertiary carbon fragment.

Dendri-PTE-$(Br)_{12}$ (MW 1428), produced a molecular ion region which was complicated by the distribution of the roughly equi-abundant bromine isotopes, ^{79}Br and ^{81}Br. The expected isotope pattern extended over a 25 dalton mass range. A computer generated isotope distribution matched very nicely with the observed experimental pattern. No major byproducts were observed. Multiple fragments were observed that correspond to fragmentation of HBr (e.g., m/z 1349 (-HBr), 1269 (-2HBr), 1189 (-3HBr), 1109 (-4HBr)).

The protonated molecular ion peak at 2285 is readily observed for d-PET-$(OH)_{36}$ (MW= 2284). As expected, H_2O fragment (MW=2267) is observed. Other fragments indicate the cleavage of the thio-alkyl bonds: 2164 (M-119), 2045 (loss of additional 119).

Overall the FAB and MALDI mass spectral data clearly indicate the desired dendrimer products are formed at each generational level with great precision and relatively low levels of side reaction.

IV. Computer Assisted Molecular Simulations

Molecular simulations were performed on a Silicon Graphics Personal Iris workstation using Polygraph modeling software (Biodesign, Inc., Pasadena, CA). The initiator core, as well as generations one through four were built and then minimized.

The procedure for energy minimization is as follows: after building the structure with the program's utilities, an initial minimization was carried out to remove the gross strain energies in the initial structure. From this local minimum energy state, a global minimum was sought using molecular dynamics. Initial modeled temperatures were relatively high, 500K, in order to provide enough energy to overcome conformational energy barriers and to give rapid motion for conformational rearrangements. The dynamics were carried out at constant total energy for fixed intervals, with periodic readjustment of the temperature back down to 500K as conformational strain energy was converted to kinetic energy. This annealing process was considered to be complete when the conformational potential energy reaches a steady state. At this point, a final energy minimization was carried out to give a structure that was deemed to be a reasonable, randomized, low energy conformation.

The energies and dimensions calculated for these low energy conformations, as well as derived values, such as surface area per end group, are reported in Table 1. Analogous simulations were performed on the previously reported poly(ether); d-PE dendrimer series.[17] Various radii as a function of generation, as well as surface area/end group were calculated for this family. Figure 12 compares these dimensions with the poly(thioether) dendrimer series. According to this comparison, it indicates there is more surface area/end groups available in the thioether series as a function of generation compared to the ether series.

Table 1: Molecular Simulations of the Poly(thioether) Dendrimers (d-PTE's)

Generation	0	1	2	3	4
Energy (J)	17.35	70.65	271.86	505.29	1191.38
Diameter (Å)	4.34	15.32	25.39	33.15	42.82
Radius (Å)	2.17	7.66	12.70	16.58	21.41
# of Atoms	17	93	309	957	2901
Surface Area ($Å^2$)	59.17	737.34	2025.23	3452.37	5760.28
End groups (Z)		12	36	108	324
Surface Area per End group ($Å^2$/Z)		61.45	56.26	31.97	17.78

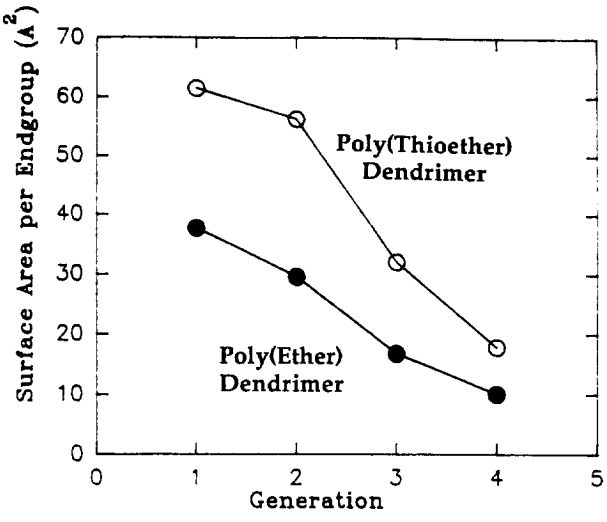

Figure 12. Comparison of Surface Areas (Å)²/Endgroup for Poly(thioether) and Poly(ether) Dendrimers

DISCUSSION

The chronological ordering and amplification patterns for the (A-GDS) synthesis of poly(thioether) dendrimers are clearly illustrated in Figure 13. The reiterative reactions (e.g., especially the mercapto anion reaction) for this poly(thioether) dendrimer series were especially facile (i.e., 80° for 4 hrs. versus 160° for 16 hrs.) compared to the previously reported poly(ether) dendrimer series. Undoubtedly, the enhanced nucleophilicity of the MTBO anion accounts for this difference. Efforts to compare the relative reaction rates of both the poly(thioether) and poly(ether) series at 160° were hampered by the fact that the sulfur containing dendrimer exhibited moderate decomposition under these conditions. Preliminary experiments have shown that the thioether groups can be oxidized to sulfoxide/sulfone type moieties in the interior. Another difference noted between the sulfur and oxygen dendrimer analogues is that steric crowding is manifested by peak broadening in the NMR spectrum of the second generation d-PTE-$(Tos)_{36}$ product, whereas, similar peak broadening in the poly(ether) (i.e., d-PE) dendrimer family does not occur until the third generation is attained. This occurs in spite of the fact that molecular simulation comparisons of the d-PTE with d-PE series suggests that there should be relatively more surface area/head group for the d-PTE series at any generational level (see Figure 12). This apparent steric congestion trend is further supported by the fact that although ideally amplified dendrimer structure was obtained for d-PTE-$(BO)_4$ → d-PTE-$(BO)_{12}$ (i.e., generations 0 → 1 → 2); attempts to advance to generation 3; d-PTE-$(BO)_{36}$ produced the non-ideally amplified structure; d-PTE-$(Br)_{24}$-$(BO)_{12}$ (see Figure 13 and Scheme II). Characterization and identification of these mutant/defective dendrimer structures by both NMR integration and MALDI mass spectroscopy clearly provides strong evidence for the "de Gennes dense packed state" at this generational level.

This type of aberrant, amplification behavior was first predicted and described by de Gennes in 1983.[18] It is consistent with our steric induced stoichiometry (SIS) hypothesis which we described in the earlier poly(ether) dendrimer work[17] and in greater detail in 1990.[5] Simply stated, there is apparently insufficient molecular space available for all 36 theoretically predicted, bicyclic orthoesters to form covalent bonds at the generation = 3a level (see Figure 13).

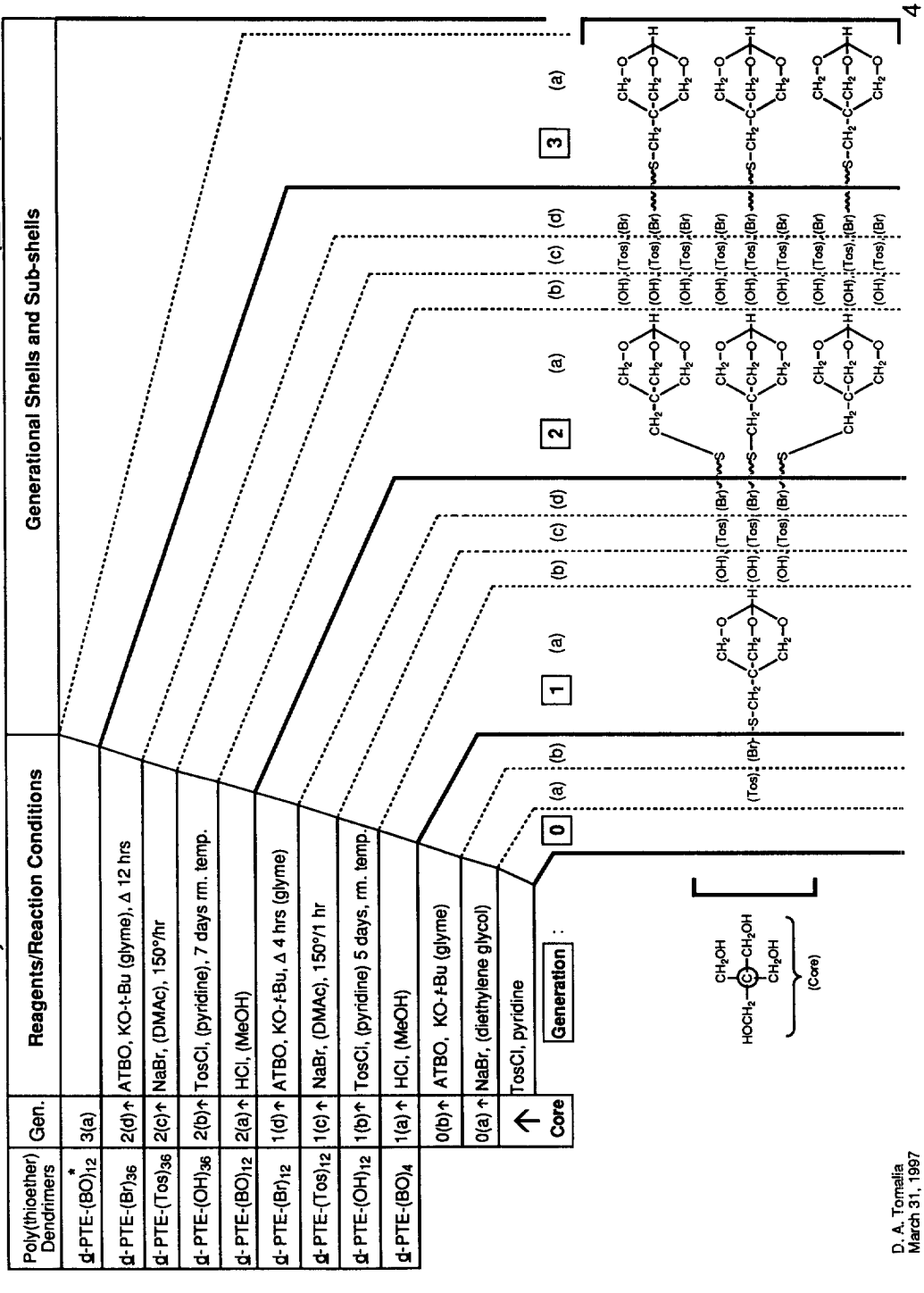
AMPLIFIED, GENEALOGICALLY DIRECTED SYNTHESIS (A-GDS)
Poly(thioether) Dendrimers
Gen.
Reagents/Reaction Conditions
Generational Shells and Sub-shells
d-PTE-(BO)12*
3(a)
d-PTE-(Br)36
2(d)↑ ATBO, KO-t-Bu (glyme), Δ 12 hrs
d-PTE-(Tos)36
2(c)↑ NaBr, (DMAc), 150°/hr
d-PTE-(OH)36
2(b)↑ TosCl, (pyridine), 7 days rm. temp.
d-PTE-(BO)12
2(a)↑ HCl, (MeOH)
d-PTE-(Br)12
1(d)↑ ATBO, KO-t-Bu, Δ 4 hrs (glyme)
d-PTE-(Tos)12
1(c)↑ NaBr, (DMAc), 150°/1 hr
d-PTE-(OH)12
1(b)↑ TosCl, (pyridine) 5 days, rm. temp.
d-PTE-(BO)4
1(a)↑ HCl, (MeOH)
0(b)↑ ATBO, KO-t-Bu (glyme)
0(a)↑ NaBr, (diethylene glycol)
TosCl, pyridine
Core
Generation :
0
1
2
3
4
(a)
(b)
(c)
(d)
(Core)
D. A. Tomalia
March 31, 1997

Figure 13

EXPERIMENTAL

General Methods - Infrared spectra were recorded on a Perkin-Elmer 983 spectrometer. ^{1}H and ^{13}C-NMR spectra were recorded on a 250 MHz WM-250 Bruker spectrometer. Chemical analyses were performed by Desert Analytics, Tucson, Arizona. Mass spectra were obtained on the V.G. ZAB-HS mass spectrometer at Dow Chemical Co. in Midland, Michigan, operating in the FAB sample introduction and ionization modes. The instrument was operated at medium resolution. FAB analysis involves dissolving a few tens of micrograms in a few microliters of Magic Bullet (3:1 DTT:DTE Aldrich) dispersant. The desorption spectrum obtained for d-PTE-$(Tos)_{12}$ involved dip sampling of a sample solution onto the emitter probe.

4-Bromomethyl-2,6,7-trioxabicyclo[2.2.2]octane (BTBO) was synthesized as described in an earlier paper.[18]

4-Acetothiomethyl-2,6,7-trioxabicyclo[2.2.2]octane (ATBO) - BTBO (11g, 50 mmole) is mixed with potassium thioacetate (60 mmole, 7.2g) in 80 mL acetone and refluxed for 1 hour. The salt is filtered off and the acetone evaporated. The product is recrystallized from ether. Yield: 98%. NMR($CDCl_3$):n 5.5 (s, 1H), 3.95 (s, 6H), 2.8 (s, 2H), 2.4 (s, 3H) ppm.

d-PTE-$(BO)_4$ - Potassium t-butoxide (2.85g, 25.5 mmole) was added to 100 mL of dry glyme under argon atmosphere. ATBO (5.2g, 25.5 mmole) and pentaerythritol tetrabromide (2.3g, 6 mmole) were added as solids and the mixture is refluxed for 4 hours, under an argon atmosphere. After cooling, methyl iodide is added as a quencher. The salts are filtered off, and most glyme is evaporated. Water is added to give a precipitate which is collected and dried. The solid is recrystallized from acetonitrile at -45°C. M.p. 260-263°C. ^{1}H-NMR(DMSO-d_6): n 5.55 (s, 1H), 3.91 (s, 6H), 2.57, 2.55 (2s, 4H) ppm. ^{13}C-NMR: δ 101.4 (formate), 69.6 (CH_2O ring), 44.6 (C_q core t), 40.3 (CH_2S next to ring), 34.8 (C_q ring), 33.3 (CH_2S core) ppm. IR(KBr): 2944, 2886, 1472, 1424, 1370, 1155, 1019, 982, 927, 858, 756 cm^{-1}. Chem. Anal. calcd for $C_{29}H_{44}O_{12}S_4$: 48.87 %C, 6.18 %H, 17.98 %S; Found: 48.82 %C, 6.22 %H, 18.26 %S.

d-PTE-$(OH)_{12}$ - A sample of d-PTE-$(BO)_4$ (1.5g, 2.1 mmole) is dissolved in a mixture of methanol (60ml) and 0.5 mL of concentrated hydrochloric acid. Methanol is distilled off slowly over 3 hours. A sticky solid is obtained after complete removal of solvent which then solidifies in a desiccator. M.p. 140-142°. ^{1}H-NMR (DMSO-d_6): δ 4.1 (OH), 3.33 (CH_2OH, s, 6H), 2.65 and 2.55 (2 br s, CH_2-S, 4H) ppm. ^{13}C-NMR (DMSO-d_6): δ 62.07($\underline{C}H_2OH$), 46.51 ($\underline{C}H_2S$), 45.4 (C quaternary), 35.65 ($\underline{C}H_2S$ inside) ppm. IR(KBr): 3339 (br, OH), 2928, 1461, 1427, 1030, 856 cm^{-1}. MS: 673 $(M+H)^+$, 655 M-H_2O, 687 M+14+H^+.

d-PTE-$(Tos)_{12}$ A sample of d-PTE-$(OH)_{12}$ (2 mmole) is dissolved in 30 mL of pyridine. At 0°C, 24 equivalents of p-toluenesulfonyl chloride (48 mmole, 9.2g) in 40 mL of pyridine are added. The mixture is allowed to stand at room temperature for 5 days, is then poured into ice water and stirred for 1 hour. The solids are filtered off and recrystallized from ethanol/chloroform (80/20). An oil is formed, which solidifies under vacuum. Yield 95%. M.p. 62-64°C. ^{1}H-NMR (DMSO-d_6): δ 7.7-7.4 (aromatic H, dd, 12H), 3.85 (CH_2OTos, s, 6H), 2.48 (CH_2S outside, s, 2H), 2.39 (Me, s, 9H), 2.13 (CH_2S core, s, 2H) ppm. ^{13}C-NMR (DMSO-d_6): δ 145, 131, 130, 127 (aromatic C), 66.9 ($\underline{C}H_2Tos$), 44.1 (C_q), 43.1 ($\underline{C}H_2S$ outside), 39.7 ($\underline{C}H_2S$ core), 21.0 (CH_3) ppm. IR(KBr): 2955, 1596, 1493, 1454, 1362, 1190, 1176, 971, 812, 789, 667, 554 cm^{-1}. Chem. Anal. Calcd for $C_{109}H_{120}O_{36}S_{16}$: 52.90%C, 4.92 %H, 20.32%S; Found 52.60%C, 4.90%H, 20.39%S. MS: 2520 M+H+, 2351 M-169(tosyl).

d-PTE-$(Br)_{12}$ - A sample of d-PTE-$(Tos)_{12}$ (1.5g, 0.6 mmole) is mixed with 28 equivalents of sodium bromide (1.7g, 17 mmole) in 10 mL dimethyl acetamide and heated at 150°C. After 1 hour, the reaction mixture is poured into water and salted out. The solid is filtered and dried. Yield: 0.7g, 83%. M.p. 165-168°. ^{1}H-NMR (DMSO-d_6): δ 3.57 (s, 6H, CH_2Br), 2.84 (s, 4H, CH_2SCH_2) ppm. ^{13}C-NMR (DMSO-d_6): δ 43.6 (C_q), 36.1 (CH_2Br) ppm. The peaks for CH_2S are hidden under the solvent peaks, this is a very dilute solution due to the insolubility of the product. IR(KBr): 2956, 2908, 1424, 1267, 1202, 1165, 834, 638, 602 cm^{-1}. Chem. Anal. Calcd. for $C_{25}H_{40}S_4Br_{12}$: 21.01%C, 2.80%H; Found 21.04%C, 2.83%H. MS: 1429 M+H+, 1349 M-HBr, 1269 M-2HBr, 1189 M-3HBr, 1109 M-4HBr.

d-PTE-$(BO)_{12}$ - Potassium t-butoxide (14 equivalents, 20 mmole, 2.2 g) is suspended in dry glyme (50 mL) under an argon atmosphere. ATBO (20 mmole, 4.1g) and d-PTE-$(Br)_{12}$ (1.4 mmole, 2 g) are added, using a solid addition funnel. The mixture is refluxed for four hours. An additional 7 equivalents of both KOtBu (1.1 g) and ATBO (2g) were added as solids refluxed overnight under argon atmosphere. After cooling, methyl iodide (5mL) is added, essentially all the glyme and the mixture was removed and water is added. The solid is filtered off and dissolved in chloroform. A small amount of ether is added, to gives a milky solution. Cooling at -8°C gives a solid which is isolated and dried. Yield: 40%. M.p. 125°C (foams, crosslinks). NMR (DMSO-d_6): δ 5.56 (s, CH, 12H), 3.92 (s, CH_2O, 72H), 2.75, 2.68, 2.61, 2.55 (4s, CH_2S, 64H) ppm. IR (KBr): 2944, 2886, 1472, 1424, 1370, 1302, 1155, 1019, 982, 927, 858, 756, 455 cm^{-1}.

d-PTE-$(OH)_{36}$ - Using the same procedure as described for the previous generation a sample of d-PTE-$(BO)_{12}$ is hydrolyzed. The bicyclic orthoester derivative is dissolved in methanol in containing in containing a trace of hydrochloric acid. The azeotrope of methyl acetate/methanol is distilled off very slowly during 2-3 hours. A solid is obtained with M.p. 53° (softening), 73°. NMR (DMSO-d_6): δ 4.21 (s, CH_2OH, 72H), 3.3 (s, H_2O and OH), 2.71, 2.67, 2.58, 2.51 (4s, CH_2S, 84H) ppm. IR(KBr): 3339 (br, OH), 2928, 1461, 1427, 1030, 856 cm^{-1}. MS: 2285 M+H+, 2299 M+14+H+, 2267 M-H_2O, 2164 M-119, 2045 M-(2x119).

d-PTE-$(Tos)_{36}$ - A sample of d-PTE-$(OH)_{36}$ (0.8 g, 0.35 mmole) is dissolved in dry pyridine (50 mL) at 0°C. p-Toluenesulfonyl chloride (60 equivalents, 21 mmole, 4 g) in 20mL of pyridine is slowly added. The mixture is allowed to stand at room temperature for an additional 5-7 days, and then poured into ice water. After 1 hour, the water is decanted, and the solids are recrystallized from ethanol/chloroform at -45°C. M.p. 90-95°C. ^{1}H-NMR (DMSO-d_6): δ 7.62, 7.59, 7.36, 7.34 (2d, aromatic, 144H), 3.79 (br s, CH_2OTos, 72H), 2.33 (s, CH_3, 108H), broad peaks at 2.2-2.5 (CH_2S) ppm. ^{13}C-NMR (DMSO-d_6): δ 146.6, 132.6, 131.4, 128.9 (aromatic), 68.1 ($\underline{C}H_2OTos$), 44 ($\underline{C}H_2S$), 22.5 (CH_3)ppm. IR(KBr): 2960, 2920, 1600, 1370, 1190, 1180, 1100, 975, 830, 820, 790, 670, 560 cm^{-1}. Chem. Anal. Calcd for $C_{337}H_{388}O_{108}S_{52}$: 51.69%C, 4.96%H, 21.27%S; Found: 51.42%C, 4.84%H, 21.02%S.

d-PTE-$(Br)_{36}$ - A sample of d-PTE-$(Tos)_{36}$ (0.3g, 0.038 mmole) is mixed with 70 equivalents of sodium bromide (2.66 mmole, 280 mg) in 10 mL dimethyl acetamide and the mixture is heated at 150° for 1 hour. The reaction mixture is then poured in water and the product is salted out, filtered, dried and recrystallized from acetonitrile. Yield: 87%. M.p. 92°. ^{1}H-NMR (DMSO-d_6): δ 3.6 (s, CH_2Br, 72H), 2.7-2.9 (3 peaks, CH_2S, 64H) ppm. IR(KBr): 2955, 2910, 1420, 1280, 1260, 835, 605 cm^{-1}. Chem. Anal. Calcd for $C_{85}H_{136}S_{16}Br_{36}$: 22.42%C, 2.99%H, 11.26%S, 63.32%Br; Found: 23.98%C, 3.17%H, 10.08%S, 59.32%Br. The chemical analysis indicates that the bromination is not complete. A calculation based on this elemental analysis shows that this product contains 34 - bromide groups versus the expected theoretical 36-Br groups.

Attempted Synthesis of d-PTE-$(BO)_{36}$ - Potassium t-butoxide (40 equivalents, 1.76 mmole, 200 mg) is suspended in dry glyme (50 mL) under argon atmosphere. ATBO (40 equiv., 1.7 mmole, 360 mg) and d-PTE-$(Br)_{36}$ (0.044 mmole, 200 mg) were added as solids. After 4 hours reflux, KOtBu (20 equiv., 100 mg) and ATBO (20 equiv., 180 mg) were added as solids, and reflux was continued overnight. After quenching with methyl iodide, water was added and the mixture stirred. The water is decanted, and the remaining solid is recrystallized from acetonitrile. A yellow solid is obtained. Careful NMR spectral analysis indicates that only 12 CH_2SCH_2-bicyclic orthoester groups are present, and 24 CH_2Br groups remain unreacted by appropriate resonance peak integrations. ^{1}H-NMR (DMSO-d_6): δ 5.56 (s, CH, 12H), 3.92 (s, CH_2O, 72H), 3.6 (br s, CH_2 Br, 48H), 2.95 - 2.55 (m , CH_2 S, 120 H) ppm.

ACKNOWLEDGMENTS

The Dow Chemical Company is gratefully acknowledged for generous financial support. We would also like to acknowledge the ARL (Army Research Laboratory), ARO (Army Research Office) and ERDEC (Edgewood Research, Development and Engineering Center). We wish to thank Drs. P. Savickas and G. Kallos (Dow Chemical Co., Analytical Department) for all FAB and MALDI mass spectroscopy data and interpretations.

REFERENCES

1. Mason, S.F. In *Chemical Evolution*; Clarendon Press: Oxford, 1991.
2. Corey, E.J.; Cheng, X.-M. *The Logic of Chemical Synthesis*; J. Wiley: New York, 1989.
3. Morawetz, H. *Polymers: The Origins and Growth of a Science*; J. Wiley: New York, 1985.
4. Elias, H.-G. *An Introduction to Polymer Science*; VCH: Weinheim, 1997.
5. Tomalia, D.A.; Naylor, A.M.; Goddard III, W.A. *Angew. Chem.* **1990**, 102(2), 119-157; *Angew. Chem. Int. Ed. Engl.*, 29(2), 138-175.
6. (a) Tomalia, D.A.; Dewald, J.R.; Hall, M.J.; Martin, S.J.; Smith, P.B. *Preprints of the 1st SPSJ International Polymer Conference*, Soc. of Polym. Sci. Japan, Kyoto, p. 65, 1984; Tomalia, D.A.; Baker, H.; Dewald, J.; Hall, M.; Kallos, G.; Martin, S.; Roeck, J.; Ryder, J.; Smith, P. *Polym. J. (Tokyo)* **1985**, 17, 117-132; *Macromolecules* **1986**, *19*, 2466-68; Tomalia, D.A.; Berry, V.; Hall, M.; Hedstrand, D.M. *Macromolecules* **1987**, *20*, 1164-67; (b) Newkome, G.R.; Yao, Z.-q.; Baker, G.R.; Gupta, V.K. *J. Org. Chem.* **1985**, *50*, 2003-2004.
7. (a) Dvornic, P.R.; Tomalia, D.A. *Current Opinion in Colloid & Interface Science* **1996**, 1, 221-235; (b) Tomalia, D.A.; Durst H.D. Genealogically Directed Synthesis: STARBURST®/Cascade Dendrimers and Hyperbranched Structures. In *Topics in Current Chemistry Vol. 165: Supramolecular Chemistry I - Directed Synthesis and Molecular Recognition*; Weber, E. Ed.; Springer-Verlag: Berlin Heidelberg, 1993; pp. 193-313; (c) Ardoin, N.; Astruc, D. *Bull. Soc. Chim. France* **1995**, 875-909; (d) Voit, B.I. *Acta Polymer.* **1995**, 46, 87-99.
8. Structural Formula of Organic Compounds Compendium. In CRC Handbook of Chemistry and Physics; Lide, D.R. Ed.; CRC Press: Boca Raton New York, 1995; pp. 331-585.
9. (a) Merrifield, R.B.; Barany G. In *The Peptides*, Vol. 2, Gross, E.; Meienhofer, J. Eds.; Academic Press: New York, 1980; (b) Merrifield, R.B. *Angew. Chem.* **1985**, 97, 801; *Angew. Chem. Int. Ed. Engl.* 24, 799; (c) Bodanszky, M. *Principles of Peptide Synthesis*; Springer-Verlag: Berlin Heidelberg, 1984; (d) Bodanzky, M; Bodanzky, A. *The Practice of Peptide Synthesis*; Springer-Verlag: Berlin Heidelberg New York, 1984.
10. (a) Tomalia, D.A.; Dvornic, P.R. Dendritic Polymers, Divergent Synthesis (Starburst Polyamidoamine Dendrimers). In *Polymeric Materials Encyl.*; Salamone, J.C. Ed.; CRC Press: Boca Raton, FL, 1996, Vol. 3, D-E, 1814-1830; (b) Dvornic, P.R.; Tomalia, D.A. *Science Spectra* **1996**, 5, 36-41.
11. Hawker, C.J.; Fréchet, J.M.J. *J. Am. Chem. Soc.* **1990**, 112, 7638-7647.
12. Newkome, G.R.; Moorefield, C.N.; Vögtle, F. In *Dendritic Molecules*; Walter, G. Ed.; VCH Publishers: New York & Weinheim, 1996.
13. Mullis, K.B.; Faloona, F.A. *Methods Enzymol.* **1987**, 155, 335.
14. Darnell, J.; Lodish, H.; Baltimore, D. *Molecular Cell Biology*; Scientific American Books: New York, 1986.
15. Dvornic, P.R.; Tomalia, D.A. *Chemistry in Britain* **1994**, 30 (8), 641-645.
16. Singer, M.; Berg, P. In *Genes & Genomes*; University Science Books: Mill Valley, CA, 1991.
17. Hall, H.K. Jr.; Padias, A.B.; McConnell, R.; Tomalia, D.A. *J. Org. Chem.* **1987**, *52*, 5305-5312.
18. Padias, A.B.; Hall, H.K. Jr. *Macromolecules* **1982**, 15, 217-223.
19. Tomalia, D.A., Dvornic, P.R. *Macromol. Symp.* **1995**, 403-428.

(*Received* 23 *June* 1997; *revised* 24 *July* 1997; *accepted* 25 *August* 1997)